4-2008

Constraining the amplitude of late Oligocene bathymetric changes in Western Ross Sea during orbitally-induced oscillations in the East Antarctic Ice Sheet: (1) Implications for glacimarine sequence stratigraphic models

Gavin B. Dunbar
University of Wellington, New Zealand, gavin.dunbar@vuw.ac.nz

T. R. Naish
University of Wellington, New Zealand

Peter J. Barrett
University of Wellington, New Zealand, peter.barrett@vuw.ac.nz

Christopher R. Fielding
University of Nebraska-Lincoln, cfielding2@unl.edu

R. D. Powell
Northern Illinois University, ross@geol.niu.edu

Published in *Palaeogeography, Palaeoclimatology, Palaeoecology* 260:1-2 (April 7, 2008), pp. 50–65 (Special issue on Antarctic cryosphere and Southern Ocean climate evolution (Cenozoic-Holocene), from 1) EGU Meeting, and 2) XXIX SCAR Meeting); doi:10.1016/j.palaeo.2007.08.018

Submitted May 24, 2007; accepted August 22, 2007; published online December 17, 2007.

Constraining the amplitude of late Oligocene bathymetric changes in Western Ross Sea during orbitally-induced oscillations in the East Antarctic Ice Sheet: (1) Implications for glacimarine sequence stratigraphic models

G. B. Dunbar,[1] T. R. Naish,[1,2] P. J. Barrett,[1] C. R. Fielding,[3] and R. D. Powell [4]

1. Antarctic Research Centre, Victoria University of Wellington, P.O. Box 600, Wellington, New Zealand
2. GNS Science, P.O. Box 30368, Lower Hutt, New Zealand
3. Department of Geosciences, University of Nebraska–Lincoln, 214 Bessey Hall, Lincoln, NE 68588-0340, USA
4. Department of Geology and Environmental Geosciences, Northern Illinois University, DeKalb, IL, 60115, USA

Corresponding author — G. B. Dunbar, email gavin.dunbar@vuw.ac.nz

Abstract
Late Oligocene shallow glacimarine sequences recovered from western Ross Sea, Antarctica by the Cape Roberts (drilling) Project display orbitally-influenced cycles of advance and retreat of a laterally-extensive ice sheet across the continental shelf, in concert with changes in contemporary water-depth. During interglacial periods, when the glacier terminated on land, the coastline was largely ice-free and wave-influenced, and sediments accumulated in hydrodynamic equilibrium with the contemporary wave-climate. Here, we present estimates of paleobathymetry from intervals of three Milankovitch-duration glacimarine sequences (9, 10 and 11) that accumulated in open ocean conditions. We utilize an approach where the percentage of mud (< 63 μm fraction) in bulk sediment is related to the wave-induced bed shear stress, and for a given wave climate, water depth (e.g. Dunbar, G. B. and Barrett, P. J., 2005. Estimating paleobathymetry of wave-graded continental shelves from sediment texture. *Sedimentology* 52, 253–269.). Particle size-derived changes in paleobathymetry for the three late Oligocene sequences were between 20–40 and 60–90 m. These water depth changes are consistent with the magnitude of contemporary global eustatic sea-level changes of 30–40 m estimated from far-field continental margin and deep-marine ocean proxy records. On the basis of our bathymetric constraints we contribute to a conceptual stratigraphic model for shallow glacimarine sequences, whose depositional architecture is controlled by a combination glacier advance and retreat and changes in relative sea-level.

Keywords: Cape Roberts Project, Oligocene, paleobathymetry, sequence stratigraphy, glaciomarine facies, Antarctica

1. Introduction

The Oligocene (c. 33–24 Ma) marks a transition from relatively ice-free "greenhouse" conditions of the Early Cenozoic to the "icehouse" world of today. Its onset coincides with one of the most significant, and widely documented changes in Earth's climate ~ 34 million years ago, that is marked by geological evidence of rapid global cooling (e.g. Hambrey et al., 1991), widespread reorganization of ocean circulation (e.g. Kennett and Stott, 1991) and the abrupt turnover of both marine and terrestrial biota (e.g. Prothero and Berggren, 1992). These events have been linked to the rapid onset of glaciation on East Antarctica (Barrett, 1987; Hambrey et al., 1991; Wise et al., 1991; Zachos et al., 1992), which initiated a long term cooling trend culminating in the bipolar glaciations of the last 3 million years. The Oligocene period was characterized by planetary temperatures 2–3 °C warmer than at present (Miller et al., 1991; Zachos et al., 2001a; Billups and Schrag, 2002), atmospheric CO_2 levels twice as high as today (Pearson and Palmer, 2000; Pagani et al., 2005) and fluctuating ice sheets on Antarctica (Barrett, 1987, 1989; Naish et al., 2001a) that appear to have been strongly modulated by variations in Earth's orbital geometry on timescales of 10^4–10^6 years — i.e. Milankovitch climate cycles (Naish et al., 2001a). Axial tilt with its 41 ka periodicity is considered to impart the most profound influence on high-latitude insolation, and therefore, the stability of polar ice sheets. Evidence for this derives mainly from oceanic oxygen isotope (δ^{18}O) records, that show a dramatic amplification of the 41 ka climate cycle beginning in the Oligocene interpreted to represent the waxing and waning of ice sheets on Antarctica and associated fluctuations in oceanic bottom waters temperatures (e.g. ice sheet amplifier of Zachos et al., 1996; Palike et al., 2004, 2006). Periods of significant Oligocene–Miocene cooling and inferred ice sheet development on Antarctica corresponding to the Oi- and Mi-events (Miller et al., 1991) have been attributed to times of comparatively rare orbital congruence between eccentricity and obliquity (e.g. Zachos et al., 2001a). These anomalies, which consist of low-amplitude variance in obliquity (a node) and a minimum in eccentricity, appear to produce extended periods (200 ky) of low seasonality orbits favorable to ice-sheet expansion. Ice-volume estimates for the Late Oligocene–early Miocene have been determined by Pekar and DeConto (2006) and Pekar et al. (2006) by applying sea-level calibrations based on reconstructions of glacio-eustatic fluctuations recorded in the New Jersey Shelf continental margin (Pekar et al., 2002) to high-resolution δ^{18}O records from ODP Site 1090 Billups et al., 2004). These calibrated records indicate that ice-volume ranged between 50% and 125% of the present day East Antarctic Ice Sheet (EAIS) during late Oligocene and most of the early Miocene (23–17 Ma) climate cycles. Maximum ice volume occurred at the early Miocene Mi-1 event (125% of the present day ice sheet). While smaller fluctuations in ice volume, of the order of 10–30 m of equivalent sea-level have been inferred for 41 ka-duration δ^{18}O cycles, the large-scale ice-volume changes reflect modulation by 100 and 400 ka-duration components, suggesting an orbitally driven dynamic EAIS existed during the late Oligocene early Miocene.

Recently, Naish et al. (2001b) presented sediment data from shallow-marine cores (Cape Roberts Project [CRP] 2/2A) in the western Ross Sea that exhibit well-dated cyclic variations, and which link the extent of the EAIS directly to orbital cycles during the Oligocene–Miocene transition, 22.5–23 million years ago. While sedimentological and faunal evidence from the cores indicated that cyclic variations in paleobathymetry were occurring in concert with ice sheet oscillations, it has hitherto not been possible to constrain the amplitude of paleobathymetric changes in these sequences, and thus assess the influence of these ice volume changes on Oligocene glacio-eustatic sea-level changes.

In this paper, we attempt to place more quantitative constraints on estimates of water depth changes during Milankovitch-duration ice sheet oscillations recorded in Cape Roberts Project sediment cores (Figure 1A), by using the particle size characteristics of the sediments. Traditional methods for reconstructing paleobathymetric changes in analogous successions utilize the paleoecology of extant faunal (mollusca, foraminifera, ostracoda) and floral (diatom) fossil assemblages (e.g. Abbott, 1997; Naish and Kamp, 1997). Unfortunately, the use of such an approach in the Oligocene Ross Sea sediment cores is hampered by relatively low species abundance, significant non-fossiliferous stratigraphic intervals, and the highly endemic nature of modern benthic communities leading to a lack of reliable modern analogues (Hannah et al., 2000; Scherer et al., 2000; Strong and Webb, 2000; Taviani et al., 2000; Watkins and Villa, 2000). Here we demonstrate that stratigraphic variations in particle size and lithofacies primarily reflect changes in wave energy at the seabed, which for a constant wave climate are dependent on water depth. We present new paleobathymetry curves for Milankovitch-duration glacimarine cycles in the Oligocene CRP-2/2A cores. Our approach utilizes a technique successfully applied to Recent and Quaternary shallow-marine sediments in Wanganui Basin, New Zealand (Dunbar and Barrett, 2005). We then discuss the controls on the stratigraphic architecture of the CRP cycles in terms of coeval water-depth and ice-margin fluctuations and propose a new facies-based sequence stratigraphic model for glaciated continental margins that integrates aspects of previous models (e.g. Fielding et al., 2000; Naish et al., 2001a; Powell and Cooper, 2002).

2. Stratigraphic intervals selected for this study and their sedimentary cyclicity

The 1500 m-thick sediment record cored by the multinational Cape Roberts Project off the Victoria Land Coast of Antarctica (Figure 1) comprises 54 uncon-

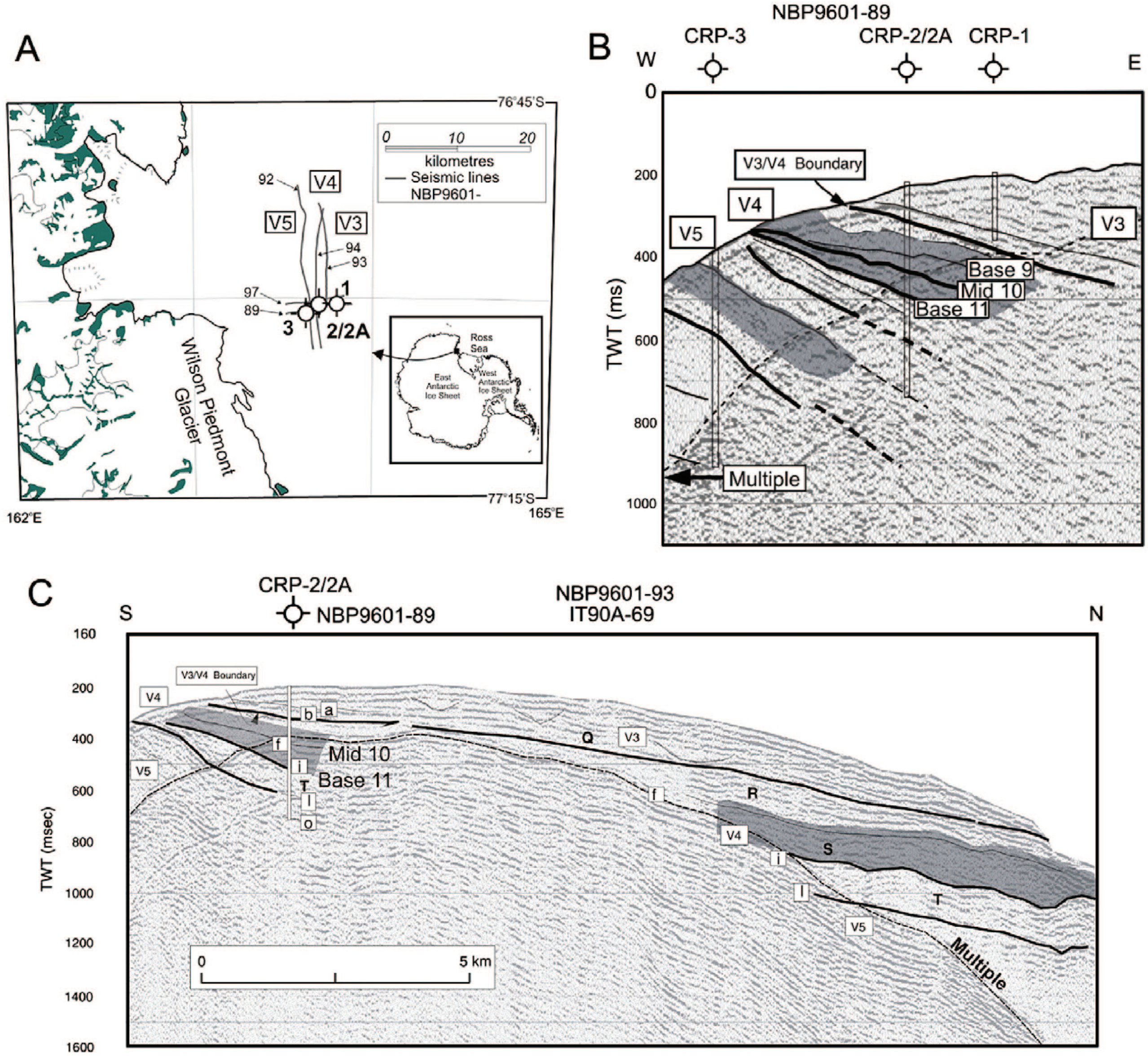

Figure 1. (A) Map of McMurdo Sound and the Cape Roberts region showing geographical setting and location of seismic lines and Cape Roberts drill sites. **(B)** Shore-normal interpreted seismic cross-section through CRP drill holes showing base of sequences, 9, 10 and 11. **(C)** Shore parallel interpreted seismic cross-section (NBP6901-93) showing the lateral extent of sequences 9, 10 and 11, which are of even thickness, and can be mapped over tens of kilometers north towards the McKay Sea Valley.

formity-bound glacimarine sequences (Naish et al., 2001b). The detail of the facies architecture and initial sequence stratigraphic interpretation is outlined for CRP-2/2A cores by Fielding et al., 2000, and is only summarized here. The thickest of these sequences (e.g. > 50 m) have also been identified in seismic reflection profiles (Fielding et al., 2001; Henrys et al., 2001). Each sedimentary cycle contains a repetitive vertical succession of lithofacies, which are interpreted to represent recurrent cycles of advance and retreat of grounded ice across the Ross Sea continental shelf, in concert with cyclical changes in water depth. The cycles identified in CRP cores have many elements in common with orbitally-controlled Plio-Pleistocene shelf cyclothems from the non-glaciated continental margins of western North Island, New Zealand (Naish and Kamp, 1997), Italy (Rio et al., 1996), Japan (Kitamura and Kondo, 1990) and California (Carter et al., 2002), suggesting significant parts of each cycle can be interpreted in terms of standard siliciclastic margin sequence stratigraphic models in which lithofacies are closely related to water depth (Figure 2).

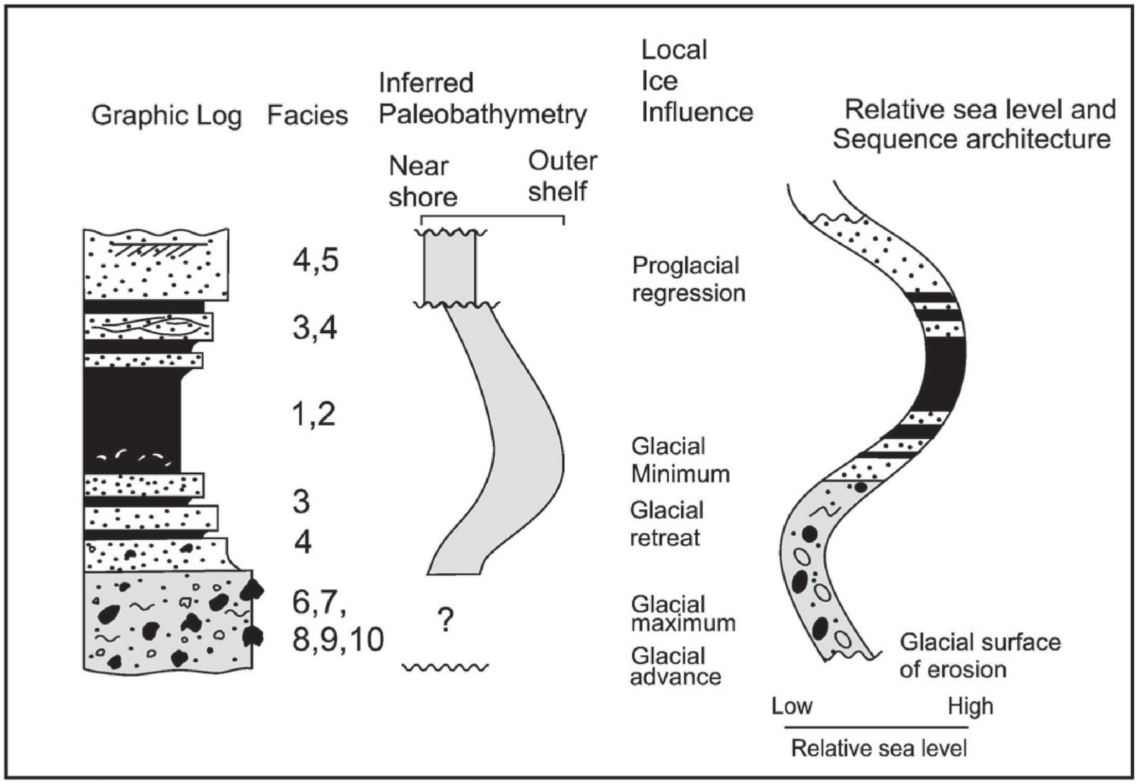

Facies	Lithology	Interpretation
1	Mudstone	-hemipelagic suspension in offshore water depths
2	Interstratified sandstone and mudstone	-range of processes: low to moderate density sediment gravity flow deposition; combined wave & current action
3	Poorly sorted (muddy) v. fine to coarse sandstone	-medium to high density sediment gravity flow deposition
4	Moderately to well sorted, stratified sandstone	- dilute tractional currents (within or about wave base to shoreface)
5	Moderately to well sorted, stratified or massive, fine to coarse sandstone	-marine currents/wave influence
6	Stratified diamictite	-subglacial or ice contact-proglacial marine deposition
7	Massive diamictite	-subglacial or ice contact-proglacial marine deposition
8	Rhythemically interstratifed sandtone and siltstone	-deposition from turbid overflow plumes associated with glacier snout efflux
9	Clast-supported conglomerate	-Deposition from a variety of processes in shallow marine environment
10	Matrix-supported conglomerate	-Deposition from a variety of processes in shallow marine environment

Figure 2. Conceptual sequence stratigraphic and facies interpretation of the Late Oligocene, Milankovitch-duration glacimarine sequences in the CRP cores (after Fielding et al., 2000; Naish et al., 2001b).

There are, however, additional facies in CRP strata that relate solely to glacimarine environments, where the primary depositional mechanism is glacier ice entering the sea (Powell et al., 2000). Each sequence has therefore been previously interpreted in terms of a standard sequence stratigraphic model where facies architecture responds to base level changes (e.g. Vail, 1987), but the model was modified to include deposition and erosion by glacial processes (Fielding et al., 2000). The sedimentary features used to arrive at these interpretations are presented in detail by Fielding et al. (2000) and Powell et al. (2000). It is important to note that constraints on paleobathymetric fluctuations, in these previous studies, were based on sedimentary structures (e.g. symmetrical ripples and hummocky cross-stratification) and sparse faunal paleobathymetric indicators (e.g. abun-

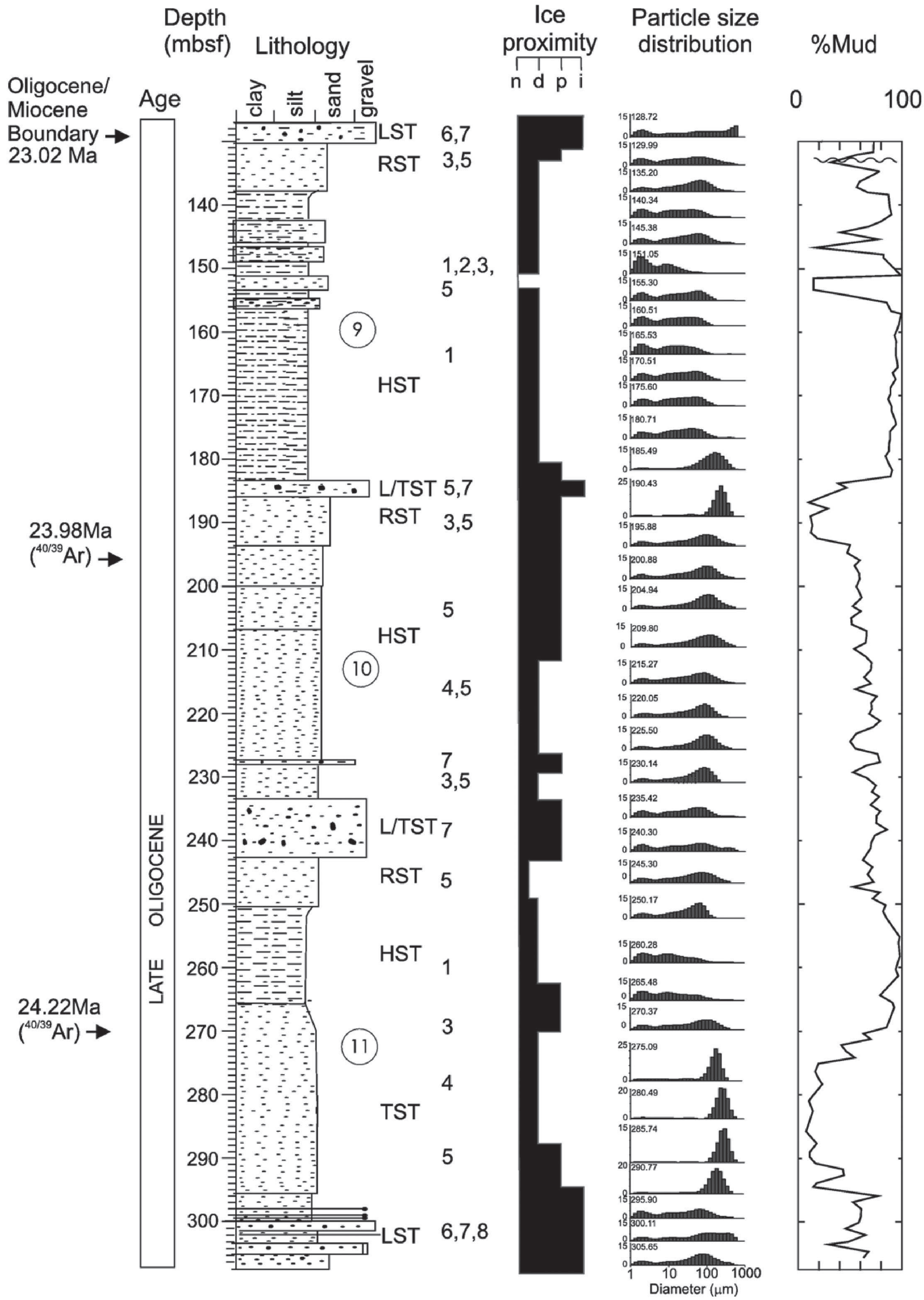

Figure 3. Summary stratigraphic log for sequences 9, 10 and 11 from CRP-2/2A shown particle size distributions and the percent mud. Ice proximity; n = non-glacial, d = distal, p = proximal, i = ice contact.

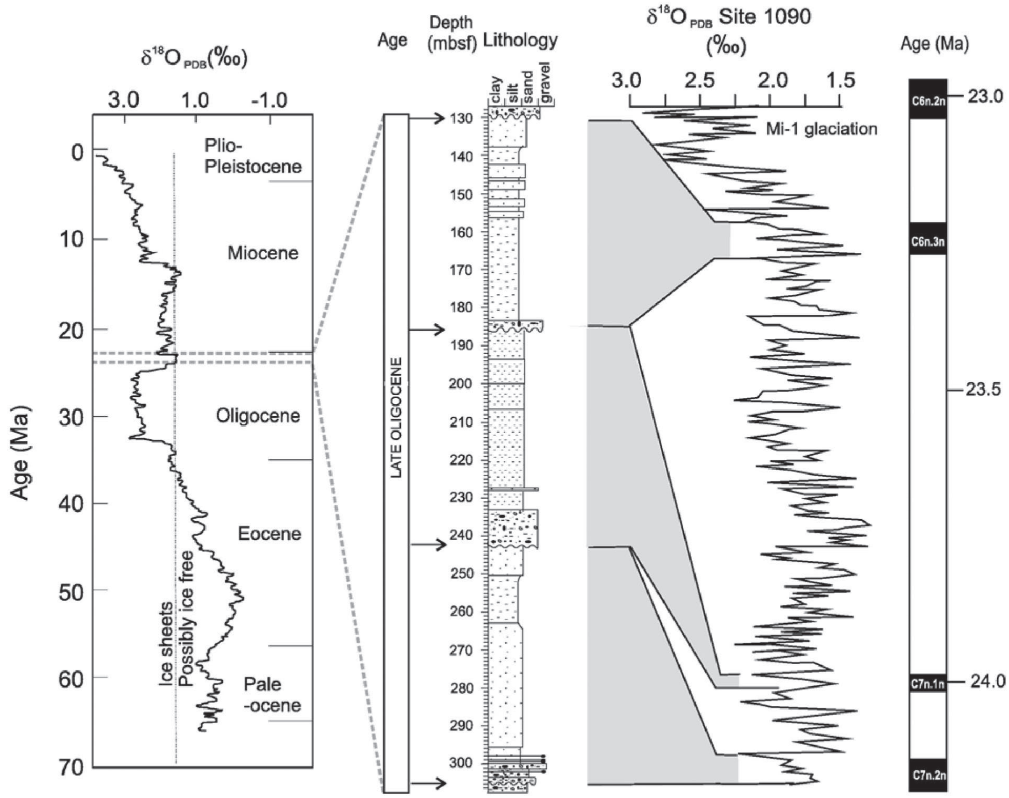

Figure 4. Correlation of the late Oligocene sequences with the astronomically-tuned, benthic oxygen isotope record of ODP Site 1090 (Billups et al., 2004). The chronostratigraphy of CRP 9,10,11 is after (Naish et al., 2008). Sequences 9 and 10 correspond to 41 ka obliquity cycles, and sequence 9 to a 100 ka cycle. Cenozoic isotope curve modified from Zachos et al. (2001b).

dance of benthic diatoms, benthic foraminifera and molluscan paleoecology) that implied water depth changes of up to ~ 50 m occurred in concert with ice margin advance and retreat cycles.

Most of the time interval spanned by the unconformity-bound sequences recovered in the CRP drill cores is not represented, owing to non-deposition and erosion through long-term tectonic influences and shorter-term glacial processes. However, intervals of relatively continuous deposition are preserved where increased rates of basin subsidence provided sufficient accommodation space (Fielding et al., 2008). One such interval has been selected for paleobathymetric analysis in this study; sequences 9, 10 and 11 between 130.27 and 306.65 m in CRP-2/2A (Figure 3). Thus, although fragmentary, the CRP record provides high-resolution windows into the history and dynamics of the EAIS and related sedimentation in the adjacent Victoria Land Basin. This stratigraphic interval comprises individual sequences that are thick enough (50–100 m) to be resolved and traced on, seismic reflection profiles (Figure 1B, C). The stratigraphic intervals also include a range of chronostratigraphic information (single crystal $^{40}Ar/^{39}Ar$ on ashes, microfossil biostratigraphy and $^{87}Sr/^{86}Sr$ ages on bioclastic carbonate) that has allowed correlation of a magnetic polarity stratigraphy to the magnetic polarity timescale and the construction of high-precision age models for the sequences (Wilson et al., 2002) for CRP-2/2A. This age model implies durations of depositional cyclicity that are consistent with orbital forcing at the 41 ka frequency band (Naish et al., 2001a).

3. Age model and correlation of Oligocene–Miocene boundary

An adjustment has been made by Naish et al. (2008) to the chronology of Late Oligocene–Early Miocene glacimarine CRP sequences published by Wilson et al. (2002), to conform with recent astrochronological calibrations of this interval of the geological timescale (e.g. Shackleton et al., 2000; Billups et al., 2004; Gradstein et al., 2004; Figure 4). The new astrochronology implies the normal polarity tephra in sequences 11 and 10 are correlated with short normal polarity chrons C7n.2n and C7n.1n, respectively. Consequently, these sequences can be uniquely matched to individual glacial–interglacial cycles on the composite oxygen isotope stratigraphy of ODP sites 929/1090 that are c. 600 ky earlier than the cycle correlation presented by Naish et al. (2001a). The normal polarity interval within Sequence 9 is now correlated with C6n.3n and implies deposition during a ~ 100–125 ky cycle, thus the Oligocene–Miocene boundary is now considered to be at the top of Sequence 9.

4. Methods and assumptions

For those intervals of sediment thought to be deposited in open marine conditions we interpret particle size variations in the sequences of the CRP core as a response to changes in wave energy at the seabed, which for a constant wave climate is dependent on water depth. The rationale is outlined briefly here and in more detail in Dunbar and Barrett (2005). In wave-dominated, inner-shelf environments, the percentage of mud (< 63 µm fraction) in bulk sediment is related to wave-induced bed shear stress, and for a given wave climate, water depth (e.g. Figure 5). Experimental observation and theoretical consideration suggests that coarse material is preferentially transported along, or near, the sea bed, whereas fine material is transported primarily in suspension. Whilst the theoretical boundary between bed and suspension transport lies around 130 µm, our observations (Dunbar and Barrett, 2005) suggest the boundary between suspension and bed transport occurs at 50–90 µm and can be reasonably approximated by percent mud. The critical level of bed shear separating the transport of sand and mud occurs at ~ 0.08 N m^{-2}, hence where this value is regularly exceeded mud will tend not to settle. Importantly, the water depth that this value occurs at varies as a function of wave height and period (i.e., wave climate), thus determining the depth at which mud will begin to accumulate and the rate at which it accumulates. However, this relationship depends on two key assumptions; first, that sediment accumulation occurred on a wave-dominated coast in equilibrium with the contemporary hydrodynamic conditions, and second, that wave climate can reasonably be estimated. The validity of these assumptions for CRP-2A sections during the Oligocene are addressed below.

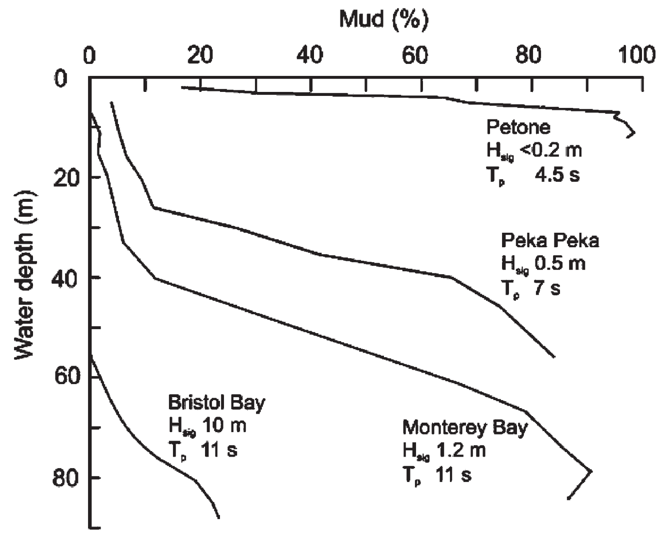

Figure 5. Percent mud plotted from published data (Dunbar and Barrett, 2005) for modern shoreface inner shelf settings of a number of different wave climates. Wave data from; Petone (Dunbar, unpublished); Peka Peka (Dunbar and Barrett, 2005); Monterey Bay, modified after (Xu, 1999); Bristol Bay (Sharma et al., 1972).

4.1. *Paleogeographic setting*

Results from a diverse range of studies suggest that coastal Victoria Land during the Oligocene experienced a cool temperate climate, with ice-free conditions at the coast during interglacial periods and glaciers advancing onto the continental shelf during glacials (Barrett, 1987; Cape Roberts Science Team, 1999, 2000). Faunal (mollusca, foraminifera, ostracoda) and floral (diatom and marine palynomorph) evidence suggests that the Cenozoic Oligocene–early Miocene strata from CRP-1 and CRP-2/2A were deposited on the continental shelf in a relatively shallow water marine environment (Cape Roberts Science Team, 1999). Palynological assemblages suggest a cool temperate climate for the Early Oligocene coastal region (mean summer daily temperature of 10–12 °C: Raine and Askin, 2001), when a low-diversity woody flora, including several species of *Nothofagus* and Podocarps, dominated vegetation. By the Miocene, climate had cooled sufficiently that vegetation was tundra-like with sparse shrub-like *Nothofagus*, for which Raine and Askin (2001) propose summer temperatures around 5–7 °C. Lithological evidence, in the form of sharp-based diamictite units, indicates that the core site was covered by grounded glaciers during cold periods. While associated sandstones and mudstones record periods of ice margin retreat, there is much evidence of rafting by sea ice or calving glacier ice. This takes the form of outsized (> 10 mm) and striated clasts, interpreted as ice-rafted debris, in all lithologies suggesting that winter surface temperatures may have been close to freezing, even during interglacial periods (Powell et al., 2000; Atkins et al., 2002). Another indication of ice rafting is the coarse sand "tail" that is also a common feature of mudstones and well-sorted fine sandstones throughout the succession (Barrett and Anderson, 2000; Powell et al., 2000).

Our understanding of the Oligocene paleogeography and geometry of the offshore sediment bodies along the Victoria Land coast is derived primarily from seismic data (Hamilton et al., 1998, 2001; Henrys et al., 2000, 2001; Fielding et al., 2006, 2008) with additional information from petrographic studies of clast provenance (Cape Roberts Science Team, 1999, 2000). We infer that these strata accumulated some kilometers off the coast as part of a laterally-extensive nearshore wedge, a geometry that is evident from an open grid of multi-channel seismic reflection profiles oriented both parallel and perpendicular to the coast (Henrys et al., 2001). During periods of glacial advance, the interior ice sheet fed through outlet glaciers to a laterally extensive marine ice terminus that extended onto the continental shelf beyond CRP drill sites (Hambrey et al., 2002; Powell et al., 2000). In periods of glacial retreat, the drill sites lay off an open marine, wave-dominated coastline broken in some places by glacier-fed river deltas and in others marine-terminating glaciers (Figure 6; Barrett, 2007).

Oligocene-age seismic sequence boundaries are laterally continuous and sub-horizontal with localized channel features (Figure 1B, C), and can be traced for many kilometers parallel to the coast. Internal seismic reflectors are often discontinuous reflecting high density and high velocity lobate bodies, probably diamictite and conglomerate interpreted as deposits of morainal banks, grounding line fans and more distal glacimarine facies that occur in the lower part of sedimentary cycles. With the exception of the thicker sequences (the focus of this paper) 9–11 in CRP2A, the resolution of the seismic data is generally too low (~ 20 m vertical) to resolve individual cycles or features within them. However, Henrys et al. (2001) were able to identify reflectors corresponding to diamictite units at the base of cycles 11 and 10 in CRP-2/2A (Figure 1B, C). These data are sufficient to show that there is, at best, very limited shore-normal channeling that could be expected from glacial or fluvial down cutting. In the dip-parallel direction, some seismic sequences preserve clinoform reflection geometries (Fielding et al., 2008), suggesting progradation of coarse clastic fans (such as deltas) into standing water during the middle and upper parts of cycles. The low-resolution reconstruction of Hamilton et al. (2001) supports this view of tabular sediment bodies now dissected by high angle normal faults.

The existence of the Transantarctic Mountains (TAM) throughout the Oligocene is inferred from the presence of material derived from several crustal blocks occurring within the TAM in CRP sediments. Exotic clasts include granite from the New Harbour Granite Complex, quartz sandstone from the Beacon Supergroup and volcanic rock fragments from the Kirkpatrick Basalts (and McMurdo Volcanic Group after 25 Ma) (Figure 1A; Smellie, 2000, 2001; Talarico et al., 2000). Therefore we believe that the Victoria Land coast was essentially a linear feature, with a large input of sediment from the TAM. During glacial periods an expanding and advancing grounded ice flowed over and beyond the drill site, but in interglacials the coast was exposed to ocean waves (albeit with a minor glacial influence as indicated by the presence of IRD; Figure 6).

4.2. Estimating wave climate

In CRP cycles the late transgressive to regressive facies successions, deposited prior to glacial overriding, are interpreted as sediment fining from inner shelf muddy-sandstone to offshore mudstone, followed by coarsening back to shoreface sandstone on a wave-graded continental shelf. The landward-coarsening pattern is driven primarily by wave-induced bed shear stress, which increases shoreward exponentially, although it also varies from place to place with wave climate, and can be influenced by sediment concentration and currents. Dunbar and Barrett (2005) investigated the relationship between bed shear stress, sediment texture and water depth by comparing percent mud and wave climate data from shore normal transects of three modern wave-graded coastal settings: Wellington Harbour (low-energy) and the Manawatu coast (moderate energy) in New Zealand and Monterey Bay in California (moderate-high energy). Samples from all three locations, as well as the high-energy Bristol Bay (Sharma et al., 1972; Figure 5) show a progressive change from poorly sorted mud offshore to well-sorted fine sand or gravel nearshore, with the sand-mud transition ranging from 3 m (low energy) to > 60 m (high energy), reflecting differences in average bed shear. Whilst there is no independent estimate of wave climate for the Victoria Land coast during the Oligocene there are sedimentological and tectonic constraints pointing to one of moderate energy. High levels of wave energy from large ocean swells running onto open coasts keep sand and mud in suspension to depths of > 50 m (e.g. Sharma et al., 1972). In such cases the shoreface is likely to be either eroding or gravelly with beaches characterized by disc-shaped clasts (Benn and Ballantyne, 1994). However, shape analysis of sequence 9–11 diamictites (Atkins, 2001) shows a lack of discs to be expected from reworking of high-energy beaches from advancing glaciers. By contrast, in low energy settings such as sheltered embayments the transition from well-sorted shoreface sand to mud occurs over a very small depth range, less than 10 m in the case of Petone (Figure 5). Under

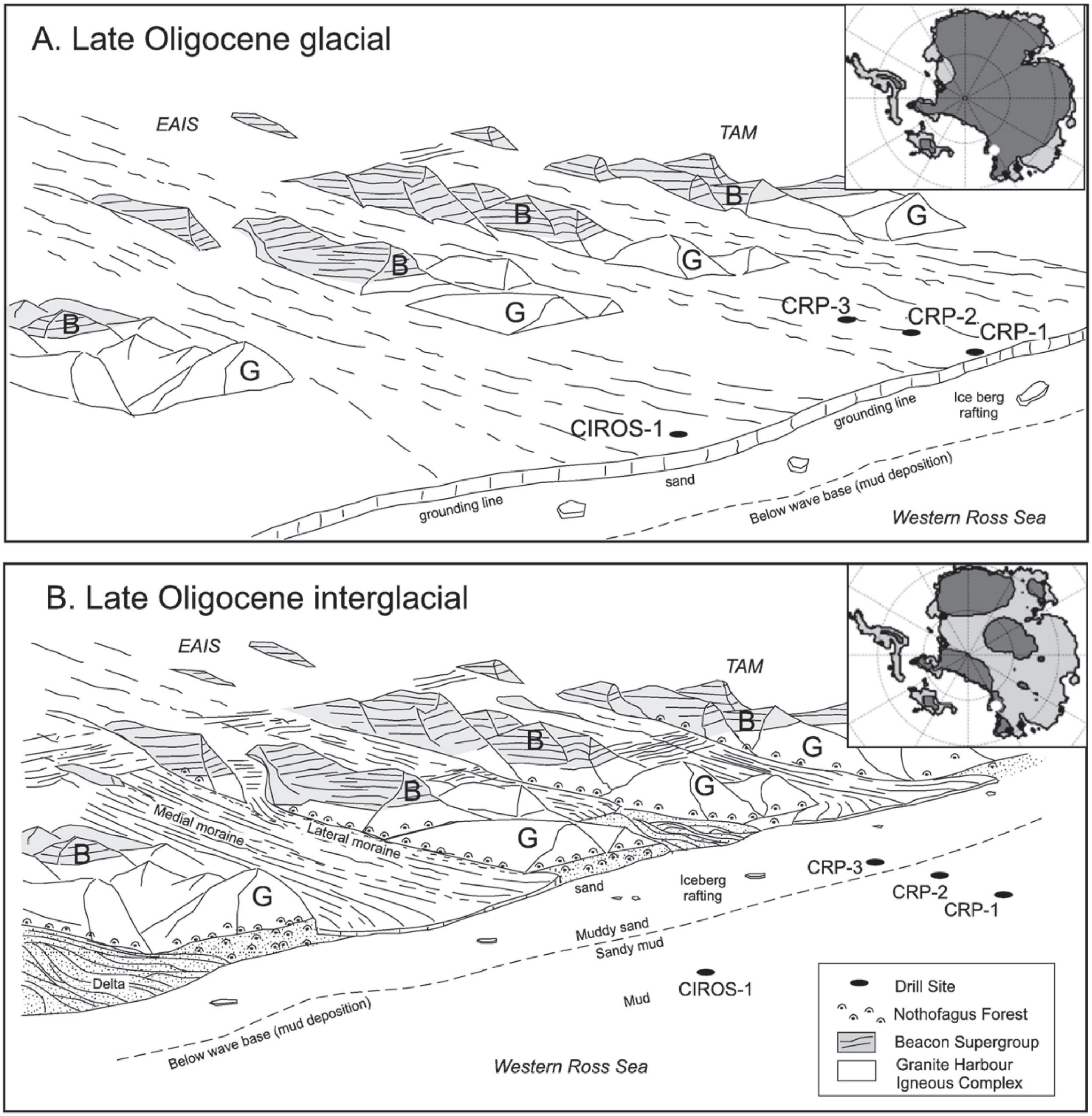

Figure 6. Schematic paleogeographic and paleoglaciaological reconstructions (DeConto et al., 2007) for the Victoria Land coast line during an late Oligocene (A) glacial period and (B) interglacial period (modified from Barrett, 2007). G = Granite, B = Beacon Supergroup.

such circumstances the accumulation of individual sand-mud sequences ~ 60 m thick would require substantial subsidence to create the necessary accommodation space. However, in the sequence stratigraphic model sand and mud are deposited during periods of reduced continental ice, along with a little isostatic rebound, making it extremely unlikely that accommodation space on this scale could be generated for the preservation of these cycles (summarized in Naish et al., 2008). The whole geographic setting of the South Victoria Land coast during the Oligocene with its long coast facing a continental shelf several hundred km across is most likely to have experienced a moderate wave climate. Therefore, we have estimated paleobathymetry using the relationship between mud and water depth at two locations, one with low moderate energy (Peka Peka) and the other with high moderate energy (Monterey Bay). These curves reveal the differences in patterns of water depth change through each of the three cycles.

4.3. Particle size

One hundred and sixty eight samples (1–3 g) were collected at 0.5–1 m-spaced intervals between 128.72 and 306.65 m in CRP-2/2A. Analyses were carried out at the Environmental Sedimentology Laboratory at James Cook University, using a Malvern Instruments Mastersizer-X laser particle size analyzer. All samples were treated with 27% H_2O_2 and checked for carbonate with 10% HCl prior to analysis. Disaggregation was carried out by crushing between wooden blocks (bulk sample) and ultrasound prior to analysis. Details of the procedure are given in Naish et al. (2001b). Experience has shown that material finer than the minimum size of the lens can create artifacts in the size distribution resulting in an artificial mode at 2.2 μm. Although this mode does not accurately reflect the size frequency distribution less than ~ 5 μm, the area under the mode is approximately proportional to the amount of sediment finer than ~ 5 μm.

5. Results

Figure 7 illustrates percentage mud and the corresponding paleobathymetric curve for sequences 9, 10 and 11 from CRP-2/2A. Paleo-water depth has fluctuated between 20–40 m and 60–90 m during deposition of these late Oligocene orbitally-controlled, glacimarine sequences. The amplitude of water depth change must be considered minimum values owing to loss of section at glacial surfaces of erosion, and loss of information in deposits from proximal glacial environments, such as at grounding-line fans and morainal banks, where diamictites, conglomerates and other proglacial deposits have not accumulated in equilibrium with local hydrodynamic setting. Maximum water depths occur within the most ice-distal offshore marine facies and correspond to times of interglacial minima. The water depth changes are 20–40% greater than predicted recently from new ice volume calibrations of the Oligocene–Miocene δ^{18}O record from ODP Site 1090 (Pekar and DeConto, 2006; Pekar et al., 2006). These calibrations utilized eustatic sea-level estimates derived from backstripping of the shallow-marine Oligocene–Miocene sequences studied on the New Jersey Margin (e.g. Kominz and Pekar, 2001; Pekar et al., 2002), and indicate that global eustatic sea-level fluctuations in the late Oligocene were between 30 and 60 m.

It is not surprising that the magnitudes of eustatic sea-level change inferred from the oxygen isotope records are 20–40% less than the maximum water depths implied from our paleobathymetric analysis of sequences 9, 10 and 11 in CRP-2/2A. This is because bathymetric changes throughout a sedimentary cycle are controlled by three independent variables: rate of eustatic sea-level change, rate of subsidence, and rate of sediment accumulation. An additional complexity at glaciated continental margins is the contribution of ice sheet loading and lithospheric depression to the total subsidence as well as the subsequent unloading and isostatic adjustment during interglacial periods. In a companion paper (Naish et al., 2008) we undertake a first-order derivation of a eustatic sea-level curve for sequence 9, by estimating values for these depositional controls. This paper demonstrates that our paleobathymetric values are consistent with, and were, primarily driven by late-Oligocene global glacio-eustatic sea-level fluctuations resulting from contemporary EAIS volume fluctuations.

6. Discussion

6.1. Implications for sequence stratigraphic models of glacimarine successions

Vertical stacking of repetitive facies successions, and cyclical patterns in sediment texture described for the CRP glacimarine sequences, have been interpreted in two ways. (1) As the advance and retreat of a glacier across the continental shelf, independent of relative sea-level fluctuations (e.g. Powell et al., 2000), or (2) as the advance and retreat of a glacier across the continental shelf, in concert with relative sea-level fluctuations (Fielding et al., 2000; Naish et al., 2001a). The bathymetric interpretation of percentage mud data presented in this paper, now allow more quantitative paleo-water depth constraints to be placed on most of the facies recognized within the CRP sequences. In all cases the qualitative sedimentary lithofacies interpretations that were based on sparse faunal and floral paleoecological data are consistent with our new water depth estimates and confirm a strong eustatic sea-level influence on sequence architecture.

Powell and Cooper (2002) presented a glacial sequence stratigraphic model based largely on seismic observations of Pleistocene successions from the cool-temperate Alaskan shelf. This model suggests some outlet/valley glaciers advance and retreat independently of eustatic sea-level fluctuations and also deposit coarsening and fining upwards facies successions well below wave base. Our previous studies of the Cenozoic glacimarine sequences from the Antarctic continental shelf in the western Ross Sea allow both the position of the grounding line and/or the shoreline (when the grounding line is subaerial) to be traced during orbitally-influenced glacio-eustatic climate cycles. These studies point strongly to a combined influence of glacial proximity

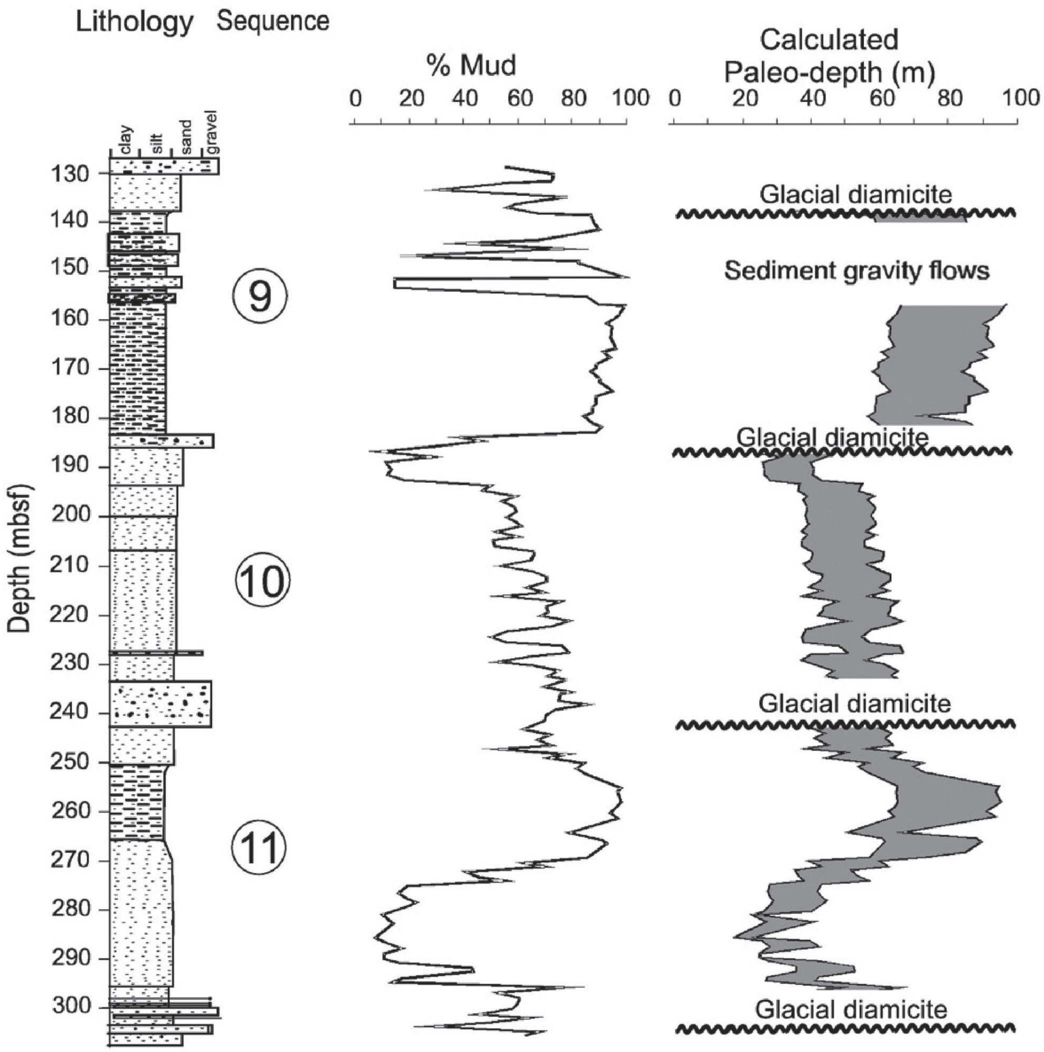

Figure 7. Percent mud and corresponding estimated paleobathymetry envelope (shaded grey) for sequences 9, 10 and 11. The shallow curve is interpolated from the moderate energy Peka Peka profile and the deeper curve from the moderate-high energy Monterey Bay profile (Figure 5). Values between points in each profile were obtained by linear interpolation.

and sea-level change on sequence architecture. In Figure 8 we present a new facies-based sequence stratigraphic model, that incorporates elements of the sea-level-independent model of Powell and Cooper (2002), and our previously published hybrid sequence stratigraphic model (e.g. Fielding et al., 2000; Naish et al., 2001b, and summarized above).

As in the previous model, each sequence begins with the *glacial surface of erosion* (GSE), which is a sharp, planar to sub horizontal erosion surface that truncates underlying deposits, and represents advance of the glacier across the seabed during falling relative sea-level. Overlying the GSE, in many cases is a sub-glacial till, comprising massive diamictite up to 10 m thick that is assigned to the lowstand systems tract (gLST). We use a lower case "g" for glacial as a prefix to denote glacimarine systems tracts. In temperate glacial systems, the subglacial till is often thin or absent (Powell and Cooper, 2002). At maximum glacial extent and the relative sea-level lowstand, the gLST may be characterized by a terminal grounding line wedge or mound of interstratified sediment gravity flow deposits and mud with dispersed clasts. The upper boundary of the gLST is marked by the *glacial retreat surface* (GRS) (Powell and Cooper, 2002), a sharp planar surface that marks the retreat of the glacier and is associated with rising base-level. The GRS replaces the *ravinement surface, or transgressive surface of erosion* (TSE) in non-glacial sequence stratigraphy (e.g. Nummedal et al., 1993). However, a TSE may develop at the shoreline if the rate of glacial retreat outpaces the rate of shoreline transgression, and the GRS is exposed to wave erosion.

The GRS is overlain by a 5–15 m-thick, fining-upwards facies assemblage deposited during ground-

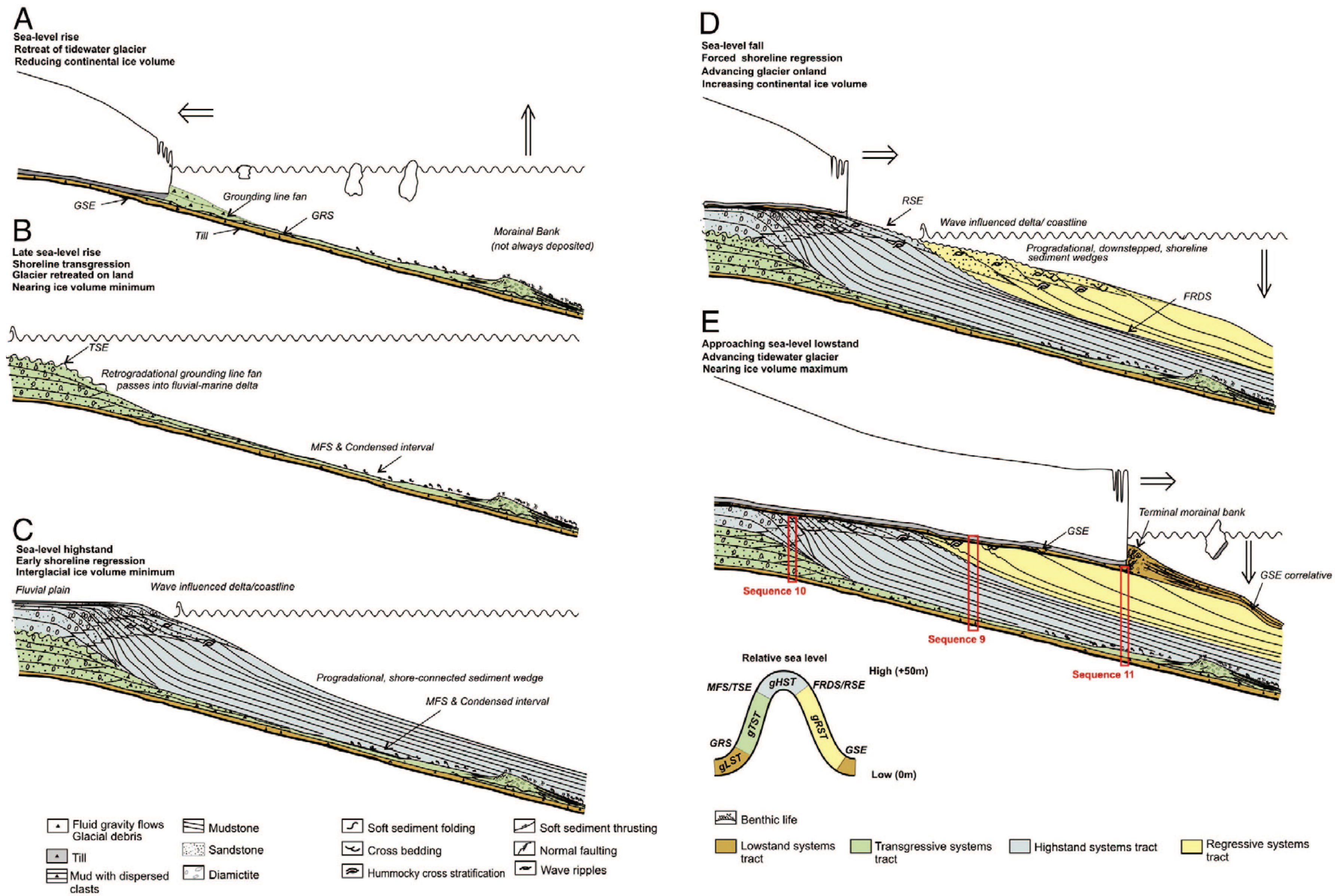

Figure 8. Glacimarine sequence stratigraphic model shows the development of facies and sequence architecture as both a function of glacial proximity and water depth change. Note relative positions of sequences 9, 10 and 11 with respect to the sequence architecture model shown in (E).

ing line retreat and bathymetric deepening, and is assigned to the transgressive systems tract (gTST). The basal deposits of the gTST comprise conglomerates and poorly sorted stratified sandstones together with stratified diamictite. Diamictites are usually associated with a range of glacimarine processes including meltwater outwash, proglacial debris-flow deposition, and melt-out. Typically, diamictite clast fabrics are weakly oriented or random, suggesting a large component of rainout debris, which in many cases, may have been remobilized in subsequent gravity flows as evidenced by syndepositional soft-sediment deformation structures, intraclasts, and clastic intrusions. The coarser-grained facies pass upwards into mud with dispersed clasts and are often capped by a sparsely fossiliferous bioturbated mudstone equivalent to the condensed section. Relatively-thick grounding-line fans have formed when the glacier terminus was stationary, or moving slowly during a punctuated retreat, whilst morainal banks represent the deposits of small re-advances during overall retreat, leaving a series of hummocky deposits, with intervening thinner ice proximal facies and lonestone-bearing mud.

An aggradational interval of massive to weakly-stratified, bioturbated, sparsely fossiliferous mudstone overlies the gTST and passes upwards and shorewards into muddy sandstone to sandstone facies. Water depths are static or gradually decrease through the mudstone, whereas the overlying sandstone facies appear markedly more gradational, shoaling to innermost shelf water depths under conditions of "normal" regression (e.g. Posamentier et al., 1992). This regressive facies succession infilled accommodation space generated on the shelf during relative sea-level rise towards the interglacial minimum and is assigned to the highstand systems tract (gHST). In offshore locations the *downlap surface* (DLS) marks the base of the HST, which is broadly coincident with the level of maximum water depth. The level of resolution provided by our paleobathymetric data is insufficient to resolve the precise position of the "peak paleo-water depth horizon" (e.g. maximum flooding). However, typically the maximum water depth in each sequence, as characterized by the highest percentage mud, corresponds to a ~ 5 m thick zone within the upper HST. The downlap surface marks a change from retrogradational to progradational stratal geometries at the top of the TST. In our drill core records it is not possible to evaluate stratal downlap. In seismic data, however, the downlap surface can be physically recognized in some cases, overlying the chaotic seismic facies of the gLST/gTST (Fielding et al., 2008). In core, the gTST/gHST (downlap surface) boundary is placed at an abruptly gradational transition between fining upwards sandstone facies of the gTST and bioturbated, massive sand facies of the gHST.

Many of the CRP-2/2A sequences include as their upper parts a sharp-based shallow-marine facies succession representing innermost shelf to shoreface progradation. These facies include moderately- to well-sorted, stratified fine sandstone, and moderately-sorted, stratified or massive, medium to coarse sandstone. They display a variety of tractional sedimentary structures including planar bedding and lamination (innermost shelf), hummocky and swaley cross-stratification (lower shoreface), high-angle cross-stratification (offshore bar), and low-angle cross-stratification (foreshore). Additionally, rare occurrences of ripple-laminated mudstone and sandstone may reflect estuarine conditions. The occurrence of sharp-based shallow-marine sands at the top of sequences, the strongly progradational character of the succession, and the subsequent truncation by overlying GSEs, are all consistent with sediments deposited during a period of falling relative sea-level, or forced regression (e.g. Posamentier et al., 1992). Where the base of the sandstone is erosional due to wave action and sediment bypassing seaward, we use the term "regressive surface of erosion" (RSE) (e.g. Nummedal et al., 1993). In more sea-ward locations, sand accumulation is continuous from the gHST into forced regressive deposits of the regressive systems tract (gRST; c.f. Naish and Kamp, 1997; Browne and Naish, 2003). We interpret these regressive sandstones as forming in a deltaic and open wave-influenced coastal depositional environment seaward of the advancing glacier. In all cases the upper portions of sequences appear to have been overrun and truncated by the subsequent advancing glacier.

Naish and Kamp (1997) and Browne and Naish (2003) have referred to this distinctive stratal package as the *regressive systems tract* (gRST), and view it as the logical counterpart to the transgressive systems tract. The lower boundary of the RST is frequently not possible to locate precisely where the transition from the underlying highstand systems tract is gradational, but typically it corresponds to a stratigraphically-condensed transition from mudstone to sandstone. Regressive systems tract sediments are markedly more progradational than those of the gHST, and step down or are inclined towards the basin.

7. Summary and conclusions

- Previous work shows that shallow glacimarine sequences recorded in CRP drill cores represent numerous cycles of advance and retreat of a laterally-extensive ice margin onto the western Ross Sea continental shelf in concert with changes in relative water depth.

- This paper demonstrates that during interglacial periods the coastline was largely ice free and wave-dominated, and these sediments are in hydrodynamic equilibrium with the contemporary wave-climate.
- For those intervals of sediment deposited in open marine conditions we interpret particle size variations in the sequences of the CRP core as a response to changes in wave energy at the seabed, which for a constant wave climate is dependent on water depth.
- In wave dominated, inner-shelf environments the percentage of mud (particles < 63 µm) in bulk sediment is related to wave-induced bed shear stress, and for a given wave climate, water depth (e.g. Dunbar and Barrett, 2005).
- Changes in paleobathymetry of Milankovitch-period duration were around 40–50 m as inferred from particle-size variations.
- Maximum water depths occur within the most ice-distal offshore marine facies and correspond to times interglacial minima.
- The water depth estimates are minimum values owing to loss of section at glacial surfaces of erosion, and loss of information in deposits from proximal glacial environments, such as at grounding-line fans and wedges and morainal banks, where diamictites, conglomerates and other proglacial deposits have not accumulated in equilibrium with local hydrodynamic setting.
- The relative water depth fluctuations inferred for Western Ross Sea glacimarine sequences are consistent with global ice volume reconstructions from paired Mg/Ca–δ^{18}O analyses (e.g. Billups and Schrag, 2002), and far-field eustatic sea-level estimates from backstripping non-glaciated continental margin shallow-marine sedimentary successions (e.g. Pekar et al., 2002), once the influences of isostasy, tectonism and sediment supply are accounted for (Naish et al., 2008).
- On the basis of these bathymetric constraints we present a conceptual stratigraphic model for shallow glacimarine sequences, the depositional architecture of which is controlled by a combination of glacier advance and retreat and changes in relative sea-level.

Acknowledgments — This work was partly financially supported by the Foundation for Research Science and Technology (FRST) contract (COX0410) to GNS and subcontract to VUW, a FRST Post-doctoral Fellowship to GBD (VUWX0003) and the Marsden Fund (Grant 04-GNS-010). This manuscript has benefited from numerous discussions with colleagues, especially Alan Orpin (NIWA).

References

Abbott, 1997 ► S. T. Abbott, Foraminiferal paleobathymetry and mid-cycle architecture of mid-Pleistocene depositional sequences, Wanganui Basin, New Zealand, *Palaios* **12** (1997), pp. 267–281.

Atkins, 2001 ► C. B. Atkins, Glacial influence from clast features in Oligocene and Miocene strata cored in CRP-2/2A and CRP-3, Victoria Land Basin, Antarctica, *Terra Antartica* **8** (2001), pp. 263–274.

Atkins et al., 2002 ► C. B. Atkins, P. J. Barrett, and S. R. Hicock, Cold glaciers erode and deposit; evidence from Allan Hills, Antarctica, *Geology (Boulder)* **30** (2002), pp. 659–662.

Barrett, 1987 ► P. J. Barrett, Oligocene sequence cored at CIROS-1, western McMurdo Sound, *New Zealand Antarctic Record* **7** (1987), pp. 1–7.

Barrett, 1989 ► P. J. Barrett, *Antarctic Cenozoic History from the CIROS-1 Drillhole, McMurdo Sound*, *DSIR Bulletin* vol. 245, DSIR Publishing, Wellington (1989), p. 254.

Barrett, in press ► P. J. Barrett, Cenozoic climate and sea level history from glacimarine strata off the Victoria Land coast, Cape Roberts Project, Antarctica. In: M. J. Hambrey, P. Christoffersen, N. F. Glasser, and B. Hubbart (eds.), Glacial Processes and products, *International Association of Sedimentologists Special Publication* **39** (2007), pp. 259–287.

Barrett and Anderson, 2000 ► P. J. Barrett and J. Anderson, Grain size analysis of samples from CRP-2/2A, Victoria Land Basin, Antarctica, *Terra Antartica* **7** (2000), pp. 373–378.

Benn and Ballantyne, 1994 ► D. I. Benn and C. K. Ballantyne, Reconstructing the transport history of glacigenic sediments: A new approach based on the co-variance of clast form indices, *Sedimentary Geology* **91** (1994), pp. 215–227.

Billups and Schrag, 2002 ► K. Billups and D. P. Schrag, Paleotemperatures and ice volume of the past 27 Myr revisited with paired Mg/Ca and ^{18}O/^{16}O measurements on benthic Foraminifera, *Paleoceanography* **17** (2002), p. 11.

Billups et al., 2004 ► K. Billups, H. Palike, J. E. T. Channell, J. C. Zachos, and N. J. Shackleton, Astronomic calibration of the late Oligocene through early Miocene geomagnetic polarity time scale, *Earth and Planetary Science Letters* **224** (2004), pp. 33–44.

Browne and Naish, 2003 ► G. H. Browne and T. R. Naish, Facies development and sequence architecture of a late Quaternary fluvial-marine transition, Canterbury Plains and shelf, New Zealand; implications for forced regressive deposits, *Sedimentary Geology* **158** (2003), pp. 57–86.

Cape Roberts Science Team, 1999 ► Cape Roberts Science Team, *Initial Report of CRP-2/2A, Cape Roberts Project, Antarctica*, *Terra Antartica* **vol. 6** (1999).

Cape Roberts Science Team, 2000 ► Cape Roberts Science Team, *Initial Report on CRP-3, Cape Roberts Project, Antarctica*, *Terra Antartica* **vol. 7** (2000).

Carter et al., 2002 ► R. M. Carter, S. T. Abbott, I. J. Graham, T. R. Naish, and P. R. Gammon, The middle Pleistocene Merced-2 and -3 sequences from Ocean Beach, San Francisco, *Sedimentary Geology* **153** (2002), pp. 23–41.

DeConto et al., 2007 ► R. DeConto, D. Pollard, and D. Harwood, Sea ice feedback and Cenozoic evolution of Antarctic climate and ice sheets, *Paleoceanography* **22** (2007), p. PA3214 ; DOI: 10.1029/2006PA001350.

Dunbar and Barrett, 2005 ► G. B. Dunbar and P. J. Barrett, Estimating palaeobathymetry of wave-graded continental shelves from sediment texture, *Sedimentology* **52** (2005), pp. 253–269.

Fielding et al., 2000 ► C. R. Fielding, T. R. Naish, K. J. Woolfe, and M. A. Lavelle, Facies analysis and sequence stratigraphy of CRP-2/2A, Victoria Land Basin, Antarctica, *Terra Antartica* **7** (2000), pp. 323–338.

Fielding et al., 2001 ► C. R. Fielding, T. R. Naish, and K. J. Woolfe, Facies architecture of the CRP-3 drillhole, Victoria Land Basin, Antarctica, *Terra Antartica* **8** (2001), pp. 217–224.

Fielding et al., 2006 ► C. R. Fielding, S. A. Henrys, and T. J. Wilson, Rift history of the western Victoria Land Basin: A new perspective based on integration of cores with seismic reflection data. In: D. K. Futterer, D. Damaske, G. Kleinschmidt, H. Miller and F. Tessensohn (eds.), *Antarctica: Contributions to Global Earth Sciences*, Springer-Verlag, Berlin (2006), pp. 309–318.

Fielding et al., 2008 ► C. R. Fielding, J. Whittaker, S. A. Henrys, T. J. Wilson, and T. R. Naish, Seismic facies and stratigraphy of the Cenozoic succession in McMurdo Sound, Antarctica: Implications for tectonic, climatic and glacial history, *Palaeogeography, Palaeoclimatology, Palaeoecology* **260** (2008), pp. 8–29; DOI: 10.1016/j.palaeo.2007.08.016.

Gradstein et al., 2004 ► F. M. Gradstein, J. G. Ogg, and A. G. Smith, Editors, *A Geologic Timescale 2004*, Cambridge University Press, New York (2004) 589.

Hambrey et al., 1991 ► M. J. Hambrey, W. U. Ehrmann, and B. Larsen, Cenozoic glacial record of the Prydz Bay continental shelf, East Antarctica. In: J. A. Barron, B. Larsen, J. G. Baldauf, C. Alibert, S. Berkowitz, S. R. Chambers, A. K. Cooper, R. E. Cranston, W. U. Dorn, W. U. Ehrmann, R. D. Fox, G. A. Fryxell, M. J. Hambrey, C. J. Jenkins, S. -H. Kang, K. W. Mehl, I. Noh, G. Ollier, A. Pittenger, C. J. Schroder, A. Solheim, D. A. Stockwell, B. Tocher, and B. R. Turner, Editors, *Proceedings of the Ocean Drilling Program, Scientific Results*, Ocean Drilling Program, College Station, TX (1991), pp. 77–132.

Hambrey et al., 2002 ► M. J. Hambrey, P. J. Barrett, and R. D. Powell In: J. A. Dowdeswell and C. O'Cofaigh, Editors, *Late Oligocene and Early Miocene Glacimarine Sedimentation in the SW Ross Sea, Antarctica: The Record from Offshore Drilling*, Geological Society of London Special Publication (2002), pp. 105–128.

Hamilton et al., 1998 ► R. J. Hamilton, C. C. Sorlien, B. P. Luyendyk, L. R. Bartek, and S. A. Henrys, Tectonic regimes and structural trends off Cape Roberts, Antarctica, *Terra Antartica* **5** (1998), pp. 261–272.

Hamilton et al., 2001 ► R. J. Hamilton, B. P. Luyendyk, C. C. Sorlien, and L. R. Bartek, Cenozoic tectonics of the Cape Roberts Rift Basin and Transantarctic Mountains Front, Southwestern Ross Sea, Antarctica, *Tectonics* **20** (2001), pp. 325–342.

Hannah et al., 2000 ► M. J. Hannah, G. J. Wilson, and J. H. Wrenn, Oligocene and Early Miocene terrestrial palynomorphs from CRP2/2A, Victoria Land Basin, Antarctica, *Terra Antartica* **7** (2000), pp. 503–512.

Henrys et al., 2000 ► S. A. Henrys, C. J. Buecker, L. R. Bartek, S. Bannister, F. Niessen, and T. Wonik, Correlation of seismic reflectors with CRP 2/2A, Victoria Land Basin, Antarctica, *Terra Antartica* **7** (2000), pp. 221–230.

Henrys et al., 2001 ► S. A. Henrys, C. J. Buecker, F. Niessen, and L. R. Bartek, Correlation of seismic reflectors with the CRP-3 drillhole, Victoria Land Basin, Antarctica, *Terra Antartica* **8** (2001), pp. 127–136.

Kennett and Stott, 1991 ► J. P. Kennett and L. D. Stott, Abrupt deep-sea warming, palaeoceanographic changes and benthic extinctions at the end of the Palaeocene, *Nature (London)* **353** (1991), pp. 225–229.

Kitamura and Kondo, 1990 ► A. Kitamura and Y. Kondo, Cyclic changes of sediments and molluscan fossil associations caused by glacio-eustatic sea-level changes during the early Pleistocene; A case study of the middle part of the Omma Formation at the type locality, *Chishitsugaku Zasshi (Journal of the Geological Society of Japan)* **96** (1990), pp. 19–36.

Kominz and Pekar, 2001 ► M. A. Kominz and S. F. Pekar, Oligocene eustasy from two-dimensional sequence stratigraphic backstripping, *Geological Society of America Bulletin* **113** (2001), pp. 291–304.

Miller et al., 1991 ► K. G. Miller, J. D. Wright, and R. G. Fairbanks, Unlocking the ice house: Oligocene–Miocene oxygen isotopes, eustasy, and margin erosion, *Journal of Geophysical Research* **96** (1991), pp. 6829–6848.

Naish and Kamp, 1997 ► T. Naish and P. J. J. Kamp, Sequence stratigraphy of sixth-order (41 k. y.) Pliocene–Pleistocene cyclothems, Wanganui Basin, New Zealand; A case for the regressive systems tract, *Geological Society of America Bulletin* **109** (1997), pp. 978–999.

Naish et al., 2001a ► T. R. Naish, P. J. Barrett, G. B. Dunbar, K. J. Woolfe, A. G. Dunn, S. A. Henrys, M. Claps, R. D. Powell, and C. R. Fielding, Sedimentary cyclicity in CRP drillcore, Victoria Land Basin, Antarctica, *Terra Antartica* **8** (2001), pp. 225–244.

Naish et al., 2001b ► T. R. Naish, K. J. Woolfe, P. J. Barrett, and G. S. Wilson *et al.*, Orbitally induced oscillations in the East Antarctic ice sheet at the Oligocene/Miocene boundary, *Nature* **413** (2001), pp. 719–723.

Naish et al., 2008 ► T. R. Naish, G. S. Wilson, G. B. Dunbar, and P. J. Barrett, Constraining the amplitude of Late Oligocene bathymetric changes in Western Ross Sea during orbitally-influenced oscillations in the East Antarctic Ice Sheet: (2) Implications for global glacio-eustasy, *Palaeogeography, Palaeoclimatology, Palaeoecology* **260** (2008), pp. 66–76 DOI: 10.1016/j.palaeo.2007.08.021.

Nummedal et al., 1993 ► D. Nummedal, G. W. Riley, and P. L. Templet, High-resolution sequence architecture; a chronostratigraphic model based on equilibrium profile studies. In: H. W. Posamentier, C. P. Summerhayes, B. U. Haq, and G. P. Allen, Editors, *Sequence Stratigraphy and Facies Associations*, Special Publication of the International Association of Sedimentologists (1993), pp. 55–68.

Pagani et al., 2005 ► M. Pagani, J. Zachos, K. H. Freeman, B. Tipple, and S. M. Boharty, Marked decline in atmospheric carbon dioxide concentrations during the Paleogene, *Science* **309** (2005), pp. 600–603.

Palike et al., 2004 ► H. Palike, J. Laskar, and N. J. Shackleton, Geological constraints on the chaotic diffusion of the solar system, *Geology* **32** (2004), pp. 929–932.

Palike et al., 2006 ► H. Palike, J. Frazier, and J. C. Zachos, Extended orbitally forced palaeoclimatic records from the equatorial Atlantic Ceara Rise, *Quaternary Science Reviews* **25** (2006), pp. 3138–3149.

Pearson and Palmer, 2000 ► P. N. Pearson and M. R. Palmer, Atmospheric carbon dioxide concentrations over the past 60 million years, *Nature* **406** (2000), pp. 695–700.

Pekar and DeConto, 2006 ► S. Pekar and R. M. DeConto, High-resolution ice-volume estimates for the early Miocene: Evidence for a dynamic ice sheet in Antarctica, *Palaeogeography, Palaeoclimatology, Palaeoecology* **231** (2006), pp. 101–109.

Pekar et al., 2002 ► S. F. Pekar, N. Christie-Blick, M. A. Kominz, and K. G. Miller, Calibration between eustatic estimates from backstripping and oxygen isotopic records for the Oligocene, *Geology (Boulder)* **30** (2002), pp. 903–906.

Pekar et al., 2006 ► S. F. Pekar, R. M. DeConto, and D. M. Harwood, Resolving a late Oligocene conundrum: Deep-sea warming and Antarctic glaciation, *Palaeogeography, Palaeoclimatology, Palaeoecology* **231** (2006), pp. 29–40.

Posamentier et al., 1992 ► H. W. Posamentier, G. P. Allen, D. P. James, and M. Tesson, Forced regressions in a sequence stratigraphic framework; Concepts, examples, and exploration significance, *AAPG Bulletin* **76** (1992), pp. 1687–1709.

Powell and Cooper, 2002 ► R. D. Powell and J. M. Cooper, A glacial sequence stratigraphic model for temperate glaciated continental shelves. In: , J. A. Dowdeswell and C. O'Cofaigh (eds.), *Glacier-influenced sedimentation on high-latitude continental margins*. Geological Society, London, Special Publication (2002), pp. 215–244.

Powell et al., 2000 ► R. D. Powell, L. A. Krissek, and J. J. M. van der Meer, Preliminary depositional environmental analysis of CRP-2/2A, Victoria Land Basin, Antarctica: Palaeoglaciological and palaeoclimatic inferences, *Terra Antartica* **7** (2000), pp. 313–322.

Prothero and Berggren, 1992 ► D. R. Prothero and W. A. Berggren, *Eocene–Oligocene climatic and biotic evolution,* Princeton University Press, New Jersey (1992) 568.

Raine and Askin, 2001 ► J. I. Raine and R. A. Askin, Terrestrial palynology of Cape Roberts Project Drillhole CRP-3, Victoria Land Basin, Antarctica, *Terra Antartica* **8** (2001), pp. 389–400.

Rio et al., 1996 ► D. Rio, J. E. T. Channell, F. Massari, M. S. Poli, M. Sgavetti, A. D'Alessandro, and G. Prosser, Reading Pleistocene eustasy in a tectonically active siliciclastic shelf setting (Crotone Peninsula, southern Italy), *Geology* **24** (1996), pp. 743–746.

Scherer et al., 2000 ► R. P. Scherer, S. M. Bohaty, and D. M. Harwood, Oligocene and lower Miocene siliceous microfossil biostratigraphy of Cape Roberts Project Core CRP-2/2A, Victoria Land Basin, Antarctica, *Terra Antartica* **7** (2000), pp. 417–442.

Shackleton et al., 2000 ► N. J. Shackleton, M. A. Hall, I. Raffi, L. Tauxe, and J. Zachos, Astronomical calibration age for the Oligocene–Miocene boundary, *Geology* **28** (2000), pp. 447–450.

Sharma et al., 1972 ► G. D. Sharma, A. S. Naidu, and D. W. Hood, Bristol Bay: Model contemporary graded shelf, *American Association of Petroleum Geologists Bulletin* **56** (1972), pp. 2000–2012.

Smellie, 2000 ► J. L. Smellie, Erosional history from the Transantarctic Mountains deduced from sand grain detrital modes from CRP-2/2A, Victoria Land Basin, *Terra Antartica* **7** (2000), pp. 545–552.

Smellie, 2001 ► J. L. Smellie, History of Oligocene erosion, uplift and unroofing of the Transantarctic Mountains deduced from sandstone detrital modes in CRP-3 drillcore, Victoria Land Basin, Antarctica, *Terra Antartica* **8** (2001), pp. 481–489.

Strong and Webb, 2000 ► C. P. Strong and P. N. Webb, Oligocene and Miocene Foraminifera from CRP-2/2A, Victoria Land Basin, Antarctica, *Terra Antartica* **7** (2000), pp. 461–472.

Talarico et al., 2000 ► F. Talarico, S. Sandroni, C. F. Fielding, and C. Atkins, Variability, petrography and provenance of basement clasts in core from CRP-2/2A, Victoria Land Basin, Antarctica, *Terra Antartica* **7** (2000), pp. 529–544.

Taviani et al., 2000 ► M. Taviani, A. G. Beu, and H. A. Jonkers, Macrofossils from CRP-2/2A, Victoria Land Basin, Antarctica, *Terra Antartica* **7** (2000), pp. 513–526.

Vail, 1987 ► P. R. Vail, Seismic stratigraphy interpretation using sequence stratigraphy, part 1: Seismic stratigraphy interpretation procedure. In: A. W. Bally, Editor, *Atlas of Seismic Stratigraphy*, AAPG, Tulsa, Oklahoma (1987), pp. 1–10.

Watkins and Villa, 2000 ► D. K. Watkins and G. Villa, Palaeogene calcareous nannofossils from CRP-2/2A, Victoria Land Basin, Antarctica, *Terra Antartica* **7** (2000), pp. 443–452.

Wilson et al., 2002 ► G. S. Wilson, M. Lavelle, W. C. McIntosh, A. P. Roberts, D. M. Harwood, D. K. Watkins, G. Villa, S. M. Bohaty, C. R. Fielding, F. Florindo, L. Sagnotti, T. R. Naish, R. P. Scherer, and K. L. Verosub, Integrated chronostratigraphic calibration of the Oligocene–Miocene boundary at 24.0 ± 0.1 Ma from the CRP-2A drill core, Ross Sea, Antarctica, *Geology (Boulder)* **30** (2002), pp. 1043–1046.

Wise et al., 1991 ► S. W. Wise Jr., J. R. Breza, D. M. Harwood, and W. Wei, Paleogene glacial history of Antarctica. In: D. W. Müller, J. A. McKenzie, and H. Weissert, Editors, *Controversies in Modern Geology; Evolution of Geological Theories in Sedimentology, Earth History and Tectonics*, Academic Press Limited, London (1991), pp. 133–171.

Xu, 1999 ► J. P. Xu, Local wave climate and long-term bed shear stress characteristics in Monterey Bay, CA, *Marine Geology* **159** (1999), pp. 341–353.

Zachos et al., 1992 ► J. C. Zachos, J. R. Breza, and S. W. Wise, Early Oligocene ice-sheet expansion on Antarctica; stable isotope and sedimentological evidence from Kerguelen Plateau, southern Indian Ocean, *Geology (Boulder)* **20** (1992), pp. 569–573.

Zachos et al., 1996 ► J. C. Zachos, T. M. Quinn, and K. A. Salamy, High-resolution (10^4 years) deep-sea foraminiferal stable isotope records of the Eocene–Oligocene climate transition, *Paleoceanography* **11** (1996), pp. 251–266.

Zachos et al., 2001a ► J. Zachos, M. Pagani, L. Sloan, E. Thomas, and K. Billups, Trends, rhythms, and aberrations in global climate 65 Ma to present, *Science* **292** (2001), pp. 686–693.

Zachos et al., 2001b ► J. C. Zachos, N. J. Shackleton, J. S. Revenaugh, H. Palike, and B. P. Flower, Climate response to orbital forcing across the Oligocene–Miocene boundary, *Science* **292** (2001), pp. 274–278.